INPUT-OUTPUT LINEARIZATION AND FRACTIONAL ROBUST CONTROL OF A NON-LINEAR SYSTEM

Valérie POMMIER[†], Patrick LANUSSE[‡], Jocelyn SABATIER[◊] and Alain OUSTALOUP[‡]

LAP-CRONE Team-Université Bordeaux I–[‡]ENSERB,[◊]IUTA and [†]LAMEFIP-ENSAM
351 Cours de la Libération-33405 Talence Cedex–France
fax: +33 (0)556 844 466
e-mail: pommier@lap.u-bordeaux.fr

Keywords: design methodologies; robust control; non-linear systems; feedback linearization; mechatronic system.

Abstract

This article deals with the association of a linear robust controller and an input-output linearization feedback for the control of a perturbed and non-linear system. This technique is applied to the control of a hydraulic system whose actuator is non-linear and whose load is time-variant. The piston velocity of the actuator needs to be controlled and a pressure-difference inner-loop is used to improve the performance. To remove the effect of the non-linearity, an input-output linearization under diffeomorphism and feedback is achieved. CRONE control, based on complex fractional differentiation, is applied to design a controller for piston-velocity loop even when parametric variations occur.

1 - INTRODUCTION

The work presented in this paper will be used for the control of the velocity of a hydraulic actuator that is part of a high-speed testing bench for mechanical structures. The difficulty of this control problem comes from the non-linearity of the actuator model and from the uncertainty on the model of the mechanical structure to be tested. So, the control strategy is based on three feedbacks: one to linearize the input-output behavior of the system, one to control the pressure-difference of the actuator, and one to control its velocity. Assuming that the hydraulic behavior is well modeled, it is linearized using diffeomorphism and feedback. CRONE control, which is a frequency-domain based methodology to design robust linear controller using complex-order differentiation, is finally applied. Considering the robustness/performance-quality trade-off, the plant perturbations are taken into account by using fully-structured frequency uncertainty domains to obtain the least-conservative controllers.

The article is organized as following. Section 2 gives a description and a model of the electrohydraulic system used to validate the control technique. Section 3 presents the control system and describes the input-output linearization. In section 4, CRONE control is introduced and applied.

2 - ELECTROHYDRAULIC SYSTEM

2.1. Description

The electrohydraulic system is part of a high-speed testing bench for mechanical structures (see Fig.1). These structures must be deformed by the electrohydraulic actuator with a velocity given in Fig.2. The actuator is a double-acting 200 mm stroke cylinder. A servo-valve fed with a hydraulic pump supplies a constant pressure. The piston rod is connected to a mechanical structure modeled by a mass-damper-spring set. The values of the structure parameters vary during the test since the structure is deformed. The cylinder chambers are each fitted with a pressure sensor. Position is provided by a LVDT sensor on the piston rod and velocity is obtained by integration of the measured acceleration.

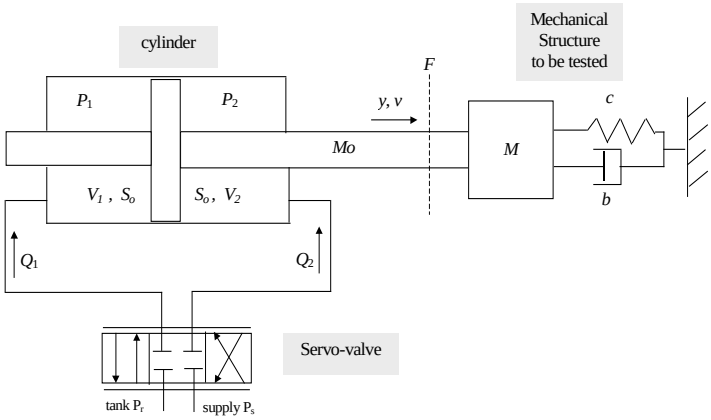

P_s: supply pressure (280 Pa)
P_r: tank pressure (1 Pa)
P_1, P_2: cylinder chamber pressures (Pa)
Q_1, Q_2: flow rate from the servo-valve to the cylinder chambers (m^3/s)
V_1 , V_2: cylinder chamber volumes (m^3)
V_o: cylinder half-volume ($5*10^{-4}$ m^3)
M_o: piston mass (50 Kg)
S_o: piston effective area ($1.53*10^{-3}$ m^2)
M: mechanical structure mass (20 Kg ±50%)
c: mechanical structure spring (100000 N/m ±50%)
b: mechanical structure viscous coefficient (200 N/m.s ±50%)
y: piston position (m)
v: piston velocity (m/s)
k : servovalve gain ($5,1.10^{-5}$)
ω_n : servovalve natural frequency (500 rad/s)
ζ_n : servovalve isodamping factor (0,4)

Fig.1 -Electrohydraulic system and mechanical structure to be tested

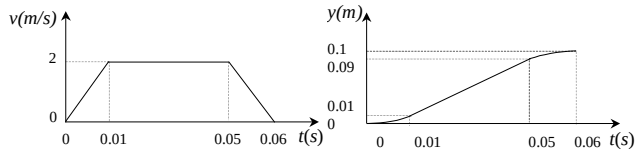

Fig.2 – Piston rod velocity and trajectory

2.2. Plant modeling

The electrohydraulic servo-valve modulates the flow rates to the cylinder chambers. The main part of the flow stage is a spool sliding in a sleeve. The spool is actuated by an electromechanical interface controlled by the input current *u*. The dynamic behavior of this interface is modeled by a two-order state space model where y_u is the image of the spool position and v_u is $\dot{y}_u$:

$$\begin{bmatrix} \dot{v}_u \\ \dot{y}_u \end{bmatrix} = \begin{bmatrix} -2\zeta_n\omega_n & -\omega_n^2 \\ 1 & 0 \end{bmatrix} \begin{bmatrix} v_u \\ y_u \end{bmatrix} + \begin{bmatrix} k\omega_n^2 \\ 0 \end{bmatrix} u \,. \tag{1}$$

The flow stage model is obtained from:

- the thermodynamic equation giving the pressure behavior:

$$\frac{V}{B}\frac{dP}{dt} + \frac{dV}{dt} = Q \,, \tag{2}$$

where *B* is the bulk isotherm modulus, and where *V*, *P* and *Q* are respectively: volume, pressure and flow rate in a cylinder chamber;

- the flow rates Q_1 and Q_2 obtained from the Bernoulli equation:

$$\begin{aligned} Q_1(y_u, P_1) &= \begin{cases} y_u\sqrt{|P_S - P_1|}\,sign(P_S - P_1) & \text{for } y_u \geq 0 \\ y_u\sqrt{|P_1 - P_r|}\,sign(P_1 - P_r) & \text{for } y_u < 0 \end{cases} \\ Q_2(y_u, P_2) &= \begin{cases} -y_u\sqrt{|P_2 - P_r|}\,sign(P_2 - P_r) & \text{for } y_u \geq 0 \\ -y_u\sqrt{|P_S - P_2|}\,sign(P_S - P_2) & \text{for } y_u < 0 \end{cases} . \end{aligned} \tag{3}$$

Static and Coulomb friction forces being neglected, the motion equation is:

$$(Mo + M)\frac{d^2y}{dt^2} = S_o(P_1 - P_2) - cy - bv \,, \tag{4}$$

where *M*, *c* and *b* are the mass, stiffness and damping parameters used to model the time-variant mechanical structure.

As volumes are: $V_1 = V_o + S_o y$ and $V_2 = V_o - S_o y$, the state-space model of the complete electrohydraulic system is obtained from equations (1), (2), (3) and (4):

$$\begin{cases} \dot{X} = f_1(X) + g(X)u & \text{for } y_u \geq 0 \\ \dot{X} = f_2(X) + g(X)u & \text{for } y_u < 0 \\ Y = h(X) \end{cases} , \tag{5}$$

with

$$X = (v_u \quad y_u \quad P_1 \quad P_2 \quad v \quad y)^T \,. \tag{6}$$

This is a one input/two outputs and six-order nonlinear model where f_1, f_2, *g* and *h* are defined by:

$$f_1(X) = \begin{pmatrix} -2\zeta_n\omega_n v_u - \omega_n^2 y_u \\ v_u \\ -\dfrac{B}{V_o + S_o y}S_o v + \dfrac{B}{V_o + S_o y}\sqrt{|P_s - P_1|}\,\text{sign}(P_s - P_1)y_u \\ \dfrac{B}{V_o - S_o y}S_o v - \dfrac{B}{V_o - S_o y}\sqrt{|P_2 - P_r|}\,\text{sign}(P_2 - P_r)y_u \\ \dfrac{1}{M_o + M}(S_o P_1 - S_o P_2 - cy - bv) \\ v \end{pmatrix} \tag{7}$$

$$f_2(X) = \begin{pmatrix} -2\zeta_n\omega_n v_u - \omega_n^2 y_u \\ v_u \\ -\dfrac{B}{V_o + S_o y}S_o v + \dfrac{B}{V_o + S_o y}\sqrt{|P_1 - P_r|}\,\text{sign}(P_1 - P_r)y_u \\ \dfrac{B}{V_o - S_o y}S_o v - \dfrac{B}{V_o - S_o y}\sqrt{|P_s - P_2|}\,\text{sign}(P_s - P_2)y_u \\ \dfrac{1}{M_o + M}(S_o P_1 - S_o P_2 - cy - bv) \\ v \end{pmatrix} \tag{8}$$

$$g(X) = \begin{pmatrix} k\omega_n^2 & 0 & 0 & 0 & 0 & 0 \end{pmatrix}^T \,, \tag{9}$$

$$h(X) = \begin{pmatrix} (P_1 - P_2) & v \end{pmatrix}^T \,. \tag{10}$$

3 - CONTROL STRATEGY

3.1. Scheme of the control system

The scheme of the control system (Fig.3) includes three feedbacks:

- ① is a feedback for the input-output linearization. The aim of this linearization is to cancel the non-linear behavior of the actuator.
- ② is a force feedback computed to quickly attenuate disturbance and perturbation on the linearized plant.
- ③ is a velocity feedback since velocity is the output to be controlled.

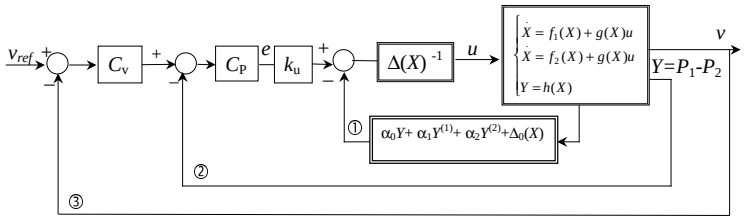

Fig.3 –Scheme of the control system

3.2. Input-output linearization under diffeomorphism and static feedback of the electrohydraulic system

The linearization is presented for positive y_u but it is similar for the negative case. e will be the linearized system input. The input-output linearization [1,2,3,4,5,6,17] uses the Lie derivatives and, L_{f1}, the Lie derivative along f_1 is given by:

$$L_{f1}(X) = \sum_{i=1}^{n} f_{1i}(X) \frac{\partial}{\partial X_i}.$$

ρ the relative degree associated with the output is defined by: $\rho = \left\{ \inf(l) \in N \ / \ L_g L_{f_1}^{l-1} h \neq 0 \right\}$. It corresponds to the first derivative of output Y that makes u appear explicitly and verifies:

$$Y^{(\rho)} = L_{f_1}^{\rho} h(X) + L_g L_{f_1}^{\rho-1} h(X)\, u \,. \qquad (11)$$

As shown by Fig.3, the output Y to be considered for the linearization is the pressure-difference.
As position y is measured, and as velocity v is obtained from the measured acceleration, the non-linear model used to computed the linearization law is a sub-part of the six-order non-linear model.

Here $X = \left(v_u \ \ y_u \ \ P_1 \ \ P_2 \right)^T$ (12)

and f_1, f_2, g and h are defined by:

$$f_1(X) = \begin{pmatrix} -2\zeta_n \omega_n v_u - \omega_n^2 y_u \\ v_u \\ -\dfrac{B}{V_o + S_o y} S_o v + \dfrac{B}{V_o + S_o y} \sqrt{|P_s - P_1|}\, \mathrm{sign}(P_s - P_1) y_u \\ \dfrac{B}{V_o - S_o y} S_o v - \dfrac{B}{V_o - S_o y} \sqrt{|P_2 - P_r|}\, \mathrm{sign}(P_2 - P_r) y_u \end{pmatrix}, \qquad (13)$$

$$f_2(X) = \begin{pmatrix} -2\zeta_n \omega_n v_u - \omega_n^2 y_u \\ v_u \\ -\dfrac{B}{V_o + S_o y} S_o v + \dfrac{B}{V_o + S_o y} \sqrt{|P_1 - P_r|}\, \mathrm{sign}(P_1 - P_r) y_u \\ \dfrac{B}{V_o - S_o y} S_o v - \dfrac{B}{V_o - S_o y} \sqrt{|P_s - P_2|}\, \mathrm{sign}(P_s - P_2) y_u \end{pmatrix} \qquad (14)$$

$$g(X) = \left(k\omega_n^2 \ \ 0 \ \ 0 \ \ 0 \right)^T \ , \qquad (15)$$

$$h(X) = \left(P_1 - P_2 \right). \qquad (16)$$

The advantage of achieving the linearization considering the pressure-difference as output is that the non-linear system is non-perturbed. Thus, the behavior of the new system to be controlled is independent of the operating points. Computation leads to $\rho = 3$. So, the decoupling term $\Delta(X)$ is given by:

$$\Delta(X) = L_g L_{f1}^{(2)} h(X), \qquad (17)$$

and the compensation term $\Delta_o(X)$ is given by:

$$\Delta_o(X) = L_{f1}^{(3)} h(X). \qquad (18)$$

Then the state feedback defined by:

$$u(X) = \frac{1}{\Delta(X)} \left[k_u e - \alpha_0 Y - \alpha_1 Y^{(1)} - \alpha_2 Y^{(2)} - \Delta_o(X) \right], \qquad (19)$$

with k_u =3.82 10^{14}, α_0 = 2.5 10^7, α_1 = 2.9 10 and α_2 = 500, transforms the non-linear system into the linearized system:

$$H(s) = \frac{k_u}{s^3 + \alpha_2 s^2 + \alpha_1 s + \alpha_0} \ . \qquad (20)$$

Usually, the input-output linearized behavior is defined by the transfer function of a ρ-order integrator. Here, the state feedback is more than a simple input-output linearizing feedback since it also contains a part of the tracking feedback. Parameter α_i, $i \in [1,3]$, are also used to avoid that the nominal ρ-order integrator system becomes a system with right half-plane poles if the actual non-linear plant is perturbed. Parameter α_i, $i \in [1,3]$, are computed so that the frequency response of $H(s)$ is comparable to the first order linear model of the nominal nonlinear plant.

4 - ROBUST CONTROLLER DESIGN

4.1. CRONE control design method

CRONE (the French acronym of "Command Robuste d'Ordre Non Entier") control system design [7,10,11,13,14] is a frequency-domain based methodolgy, using complex fractional differentiation [8,9,15,16]. It permits the robust control of perturbed plants using the common unity feedback configuration. It consists on determining the nominal and optimal open-loop transfer function that guaranties the required specifications. While taking into account the plant right half-plane zeros and poles, the controller is then obtained from the ratio of the open-loop frequency response to the nominal plant frequency response. Three Crone control generations have been developed, successively extending the application fields. Crone control design has already been applied to unstable or non-minimum-phase plants, plants with bending modes [OUS 95b], and digital control problems. In this paper, only the principle of the third generation is given. The interests of Crone control system design are multiple. The use of complex fractional differentiation permits to define the open-loop transfer function with few high-level parameters. The optimization problem that leads to the optimal transfer function to meet the specifications is thus easier to solve. Moreover, Crone control design takes into account the genuine plant perturbation without over-estimation, then better performance can be obtained.

The third generation Crone method is based on a particular Nichols locus called a *generalized template* and defined by an any-direction straight line segment around open-loop gain crossover frequency ω_{cg} (Fig.4). This generalized template is based on the real part (with respect to imaginary unit i) of complex fractional integration:

$$\beta(s) = \left[\cosh\left(b \frac{\pi}{2} \right) \right]^{-1} \Re_{/i} \left[\left(\frac{\omega_{cg}}{s} \right)^n \right], \qquad (21)$$

with $n = a + ib \in \mathbb{C}_i$ and $s = \sigma + j\omega \in \mathbb{C}_j$. In the Nichols chart at frequency ω_{cg}, the real order a determines the phase

placement of the template, and then the imaginary order b determines its angle to the vertical.

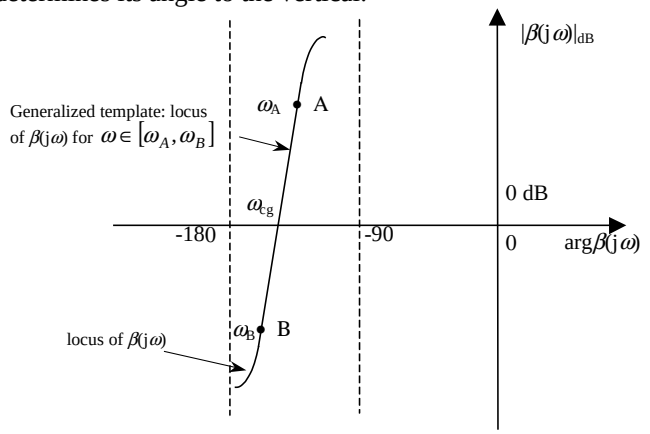

Fig.4 - Representation in the Nichols chart of the generalized template by an any-direction straight line segment

In the version of third generation Crone control design used in this article, the open-loop transfer function defined for the nominal state of the plant, $\beta_o(s)$, takes into account the control specifications at low and high frequencies and a set of band-limited generalized templates around resonant frequency ω_r. Thus $\beta_o(s)$ is defined by:

$$\beta_0(s) = K\left(\frac{\omega_{-N^-}}{s}+1\right)^{n_l}\frac{1}{(1+s/\omega_{N^++1})^{n_h}} \prod_{-N^-}^{N^+}\left(\frac{1+s/\omega_{k+1}}{1+s/\omega_k}\right)^{a_k}\left(\Re_{/i}\left[\left(C_k\frac{1+s/\omega_{k+1}}{1+s/\omega_k}\right)^{ib_k}\right]\right)^{-\mathrm{sign}(b_k)}, \quad (22)$$

where

$$C_0 = \left[\left(1+\omega_r^2/\omega_0^2\right)/\left(1+\omega_r^2/\omega_1^2\right)\right]^{1/2} \quad (23)$$

and

$$C_k = \left[\omega_{k+1}/\omega_k\right]^{1/2} \text{ for } k \neq 0 \cdot \quad (24)$$

K ensures a gain of 0 dB at ω_{cg}, the order n_l fixes the steady state behavior of the closed-loop system at low frequencies, and the value of n_h has to be chosen as equal to or greater than the high-frequency order of the plant.

Crone control design guaranties the robustness of both stability margins and performance, and particularly the robustness of the maximum M of the complementary sensitivity function magnitude. Let M_r be the required magnitude peak of the complementary sensitivity function for the nominal parametric state of the plant. An indefinite number of open-loop Nichols locus can tangent the Nichols magnitude contour of graduation M_r. Also, for uncertain plants, parametric variations lead to variations of M. Thus, an open-loop Nichols locus is defined as optimal if the generalized template around ω_t tangents the M_r Nichols magnitude contour for the nominal state and if it minimizes the variations of M for the other parametric states. By minimizing the cost function $J = (M_{max} - M_r)^2$ where M_{max} is the maximal value of magnitude peaks M, the optimal open-loop Nichols locus positions the uncertainty domains correctly, so that they overlap the low stability margin areas as little as possible. The minimization of J is carried out under a set of shaping constraints on the four usual sensitivity functions. Once the optimal open-loop Nichols locus is obtained, the controller $C_f(s)$ deduced from the ratio of $\beta_o(s)$ to the nominal plant function transfer is a fractional transfer function with fractional order. The design of the achievable controller consists in replacing $C_f(s)$ by a rational controller $C_r(s)$ which has the same frequency response.

4.2. Electrohydraulic-system control

Two controllers need to be designed. As the linearized plant $(P_1\text{-}P_2)(s)/E(s) = H(s)$ is assumed to be non-perturbed, a common PID controller is designed for the pressure-difference inner-loop. As the control system will be digital, and as Crone design, used for the robust outer-loop, is a continuous frequency-domain approach, the digital control design problem is transformed into a pseudo-continuous problem using the bilinear w-transformation defined by:

$$z^{-1} = \frac{1-w}{1+w} \quad \text{with } w=jv \text{ and } v = \tan\left(\frac{\omega T_s}{2}\right), \quad (25)$$

where T_s is the 0.2 ms sampling period.

Then, the PID transfer function used in the inner-loop is:

$$C_p(w) = C_0\left(\frac{v_i}{w}+1\right)\left(\frac{1+w/v_1}{1+w/v_2}\right)^N\frac{1}{1+w/v_f}. \quad (26)$$

Pseudo-frequencies v_i and v_f are related to integral and low-pass effect. Gain C_0, pseudo-frequencies v_1 and v_2, and integer order N are computed to ensure a 50° phase-margin and a 0.3 open-loop gain crossover pseudo-frequency. Then the PID parameters are:
$v_i = 0.06$; $v_1 = 0.09$; $v_2 = 1$ $v_f = 1.5$; $N = 3$; $C_0 = 1.73\ 10^{-6}$.

The robust controller of the velocity outer-loop is designed now. The Crone open-loop transfer function to be optimized is:

$$\beta_0(w) = K\left(\frac{v_{-N^-}}{w}+1\right)^{n_l}\frac{f(w)}{\left(1+w/v_{N^++1}\right)^{n_h}} \prod_{-N^-}^{N^+}\left(\frac{1+w/v_{k+1}}{1+w/v_k}\right)^{a_k}\left(\Re_{/i}\left[\left(C_k\frac{1+w/v_{k+1}}{1+w/v_k}\right)^{ib_k}\right]\right)^{-\mathrm{sign}(b_k)}, \quad (27)$$

where $f(w)$ is a function that takes into account the two plant right half-plane zeros closed to $v = +1$ which appeared when the bilinear w-transformation has been applied.

Here, optimization uses $N^+ = N^- = 1$, so a set of three band-limited generalized templates is used. The behavior of the open-loop transfer function at low and high frequencies is fixed with: $n_l = 2$ and $n_h = 4$. The required magnitude peak M_r

chosen for the nominal plant is 1dB and the constraints on the sensitivity functions are given by:

- the maximum plant input (100mA),
- the Fourier transform of the required trajectory,
- the maximum magnitude T_{max} of the complementary sensitivity function set at 3 dB,
- the maximum magnitude S_{max} of the sensitivity function set at 6dB.

Fig.5 and Fig.6 show the optimal open-loop Nichols and lin-log Nyquist loci. The optimal parameters position the frequency uncertainty domains to minimize the variation of the M magnitude peak. Then maximal value of sensitivity functions are M_{max} = 1.3dB and S_{max} = 6dB. The optimal resonant frequency is 0.05.

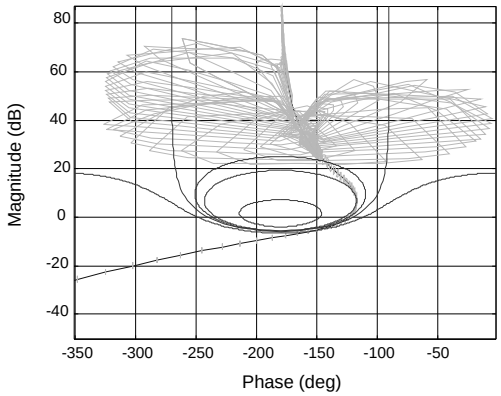

Fig.5 - Optimal open-loop Nichols and uncertainty domains

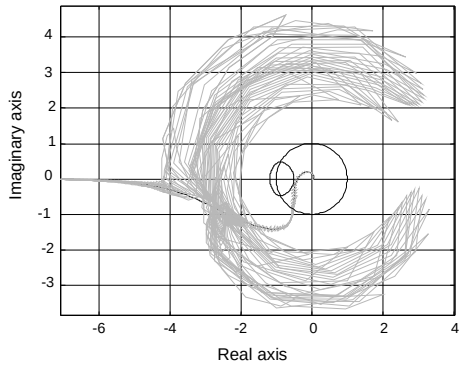

Fig.6 - Lin-log Nyquist loci and uncertainty domains

The computed pseudo-continuous rational controller obtained for the velocity feedback is nine-order filter:

$$C_v(w) = 7.94\left(1+26.67w+\frac{w^2}{9.10^{-6}}\right)\left(1+\frac{w}{0.011}\right)\left(1+7.5758w+\frac{w^2}{0.0174}\right) \quad (28)$$
$$\left(1+0.65w+\frac{w^2}{0.38}\right)w^{-3}\left(1+\frac{w}{0.069}\right)^{-4}\left(1+\frac{w}{0.3}\right)^{-1}\left(1+\frac{w}{80}\right)^{-1}.$$

The digital controllers $C_P(z^{-1})$ and $C_v(z^{-1})$ are obtained from $C_P(w)$ and $C_v(w)$ using the inverse w-transformation defined above.

Fig.7 presents the simulated output v with the Crone controller for the nominal mechanical structure. This result is compared with that obtained with a PID controller computed to have the same gain cross-over frequency and defined by:

$$C_{PID}(w) = \frac{2.174.10^7\left(1+\frac{w}{0.02}\right)}{\frac{w}{0.02}\left(1+\frac{w}{0.125}\right)} \quad (29)$$

Crone controller gives better results since the overshoot is less important than with the PID as the Crone approach permits to manage phase margin and also other stability margins as gain margin, magnitude peaks,...

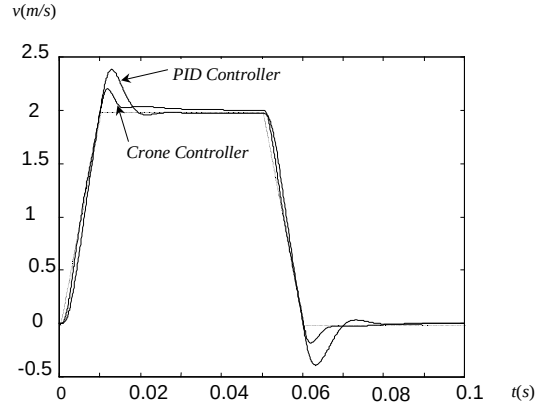

Fig.7 - Simulated controlled output for the nominal mechanical structure with the Crone controller and with a PID controller

In Fig.8, the simulated output is shown for three different mechanical structure (minimal, nominal and maximal values of the parameters) and certifies that the Crone control system is robust.

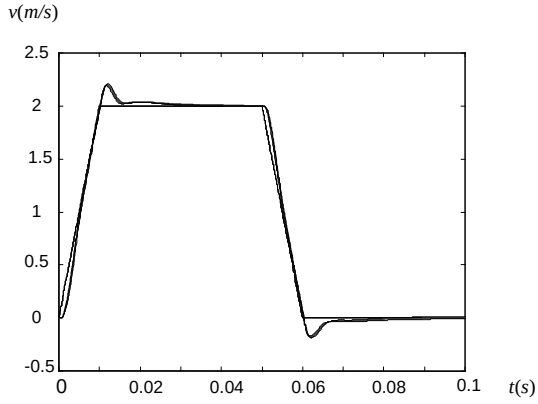

Fig.8 - Simulated controlled output for three different mechanical structures with the Crone controller

In the case of maximal values of the mechanical structure parameters, Fig.9 shows that the plant input u is less than 100 mA. Thus, the plant is not too much solicited. For other loads, plant inputs are similar.

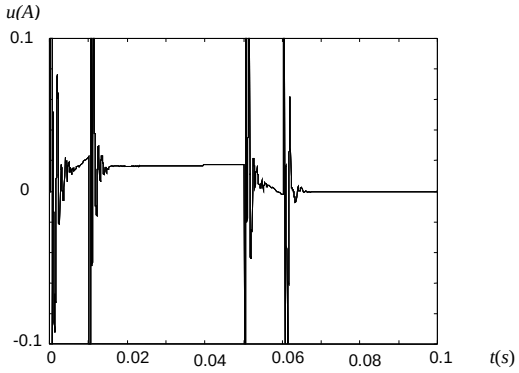

Fig.9 - Plant input

A further simulation is achieved to verify the behavior of the control system faced with a quick variation of the stiffness parameter. The initial value of the stiffness is 150000N/m and its final value is 50000N/m. Moreover, the initially neglected non-linear friction force of the hydraulic cylinder is now modeled by a 700N static friction and a 500N coulomb friction. Fig.10 shows that the tracking remains very good and that the effect of the perturbation is very-well rejected.

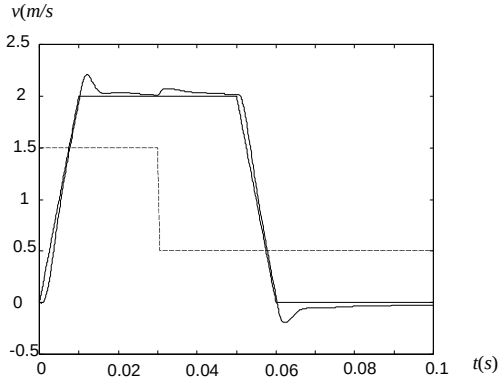

Fig.10 - Simulated controlled output with a quick variation of the stiffness parameter ($c/10^5$ - -) and non-linear friction force

5 - CONCLUSION

The robust control of a non-linear mechatronic plant with time-variant parameters can be designed using both an input-output linearizing feedback and a linear robust control system. The linear reference model used by the input-output linearizing method must be chosen carefully. In the case of an hydraulic actuator, a pressure-difference inner-loop improved significantly the disturbance rejection. Crone control design (based on fractional differentiation) permits the uncertainty of the perturbed plant to be taken into account through a structured description which is less pessimistic than most of the other robust control design approaches. Final results demonstrate the efficiency of the proposed control-system design method.

References

[1] X. Brun, M. Belghardi, S. Sesmat, D. Thomasset, and S. Scavarda, , "Control of an electropneumatic actuator, comparison between some linear and non linear control laws", Journal of systems and control engineering - special issue “Controls in fluid power system”, Vol.213, N°15, pp.387-406, (1999)

[2] D. Claude, M. Fliess and A. Isidori, Immersion directe et par découplage d'un système non linéaire dans un linéaire, *Compte-rendus de l'Académie des Sciences*, Paris, (1983).

[3] A.J. Fossard, D. Normand-Cyrot (1997), “Nonlinear Systems-Control”, Vol.3 , Chapman&Hall and Masson., (1997)

[4] A. Isidori, “Nonlinear control systems”, Springer Verlag, 2nd edition, (1989).

[5] M. Krstic, I. Kanellakopoulos and P. V. Kokotovic, *Nonlinear and Adaptive Control Design*, Wiley, New York, (1995).

[6] I.D. Landau, D. Rey, A. Karimi, A. Voda and A. Franco , « A Flexible Transmission System as a Benchmark for Robust Digital Control », European Journal of Control, Vol.1, n°2, (1995).

[7] K.S. Miller and B. Ross, An introduction to the fractional calculus and fractional differential equations, *John Wiley & Sons Inc.*, New York, (1993)

[8] K.B. Oldham and J. Spanier, The fractional calculus, *Academic Press*, New York, (1974).

[9] A. Oustaloup, The CRONE control, *ECC’91* Grenoble, France, (1991).

[10] A.Oustaloup, P. Lanusse and B. Mathieu, Robust control of SISO plants: the CRONE control, *ECC'95*, Rome, Italia, (1995).

[11] A. Oustaloup, B. Mathieu and P. Lanusse, The CRONE control of resonant plants: application to a flexible transmission, *European Journal of Control*, Vol. 1, pp. 113-121, (1995).

[12] A. Oustaloup et B. Mathieu, La commande CRONE : du scalaire au multivariable, *Editions HERMES*, Paris, (1999).

[13] A. Oustaloup, J. Sabatier and P. Lanusse, From fractal robustness to the CRONE Control, *Fractional Calculus and Applied Analysis: An international Journal for Theory and Applications*, Vol. 2, n° 1, (1999).

[14] A. Oustaloup, F. Levron, F. Nanot. and B. Mathieu, Frequency band complex non integer differentiator: Characterization and synthesis, *IEEE Transactions on Circuit and Systems*, Vol 47, n° 1, p 25-40, (2000)

[15] S.G. Samko, A.A. Kilbas and O.I. Marichev, Fractional integrals and derivatives, *Gordon and Breach Science Publishers*, (1993).

[16] Slotine & Li, “Applied Nonlinear Control”, Prentice-Hall, (1991).